

RESEARCH

Open Access



Quercetin regulates pulmonary vascular remodeling in pulmonary hypertension by downregulating TGF- β 1-Smad2/3 pathway

Rui-Juan Gao^{1,2}, Nigala Aikeremu², Nan Cao³, Chong Chen⁴, Ke-Tao Ma^{2,5,6}, Li Li⁷, Ai-Mei Zhang^{8*} and Jun-Qiang Si^{2,5,6,9*}

Abstract

Background Pulmonary arterial hypertension (PAH) is a worldwide challenging disease characterized by progressive elevation of pulmonary artery pressure. The proliferation, migration and phenotypic transformation of pulmonary smooth muscle cells are the key steps of pulmonary vascular remodeling. Quercetin (3,3', 4', 5, 6-pentahydroxyflavone, Que) is a natural flavonol compound that has antioxidant, anti-inflammatory, anti-tumor and other biological activities. Studies have shown that Que has therapeutic effects on PAH. However, the effect of quercetin on pulmonary vascular remodeling in PAH and its mechanism remain unclear.

Methods and results In vivo, PAH rats were constructed by intraperitoneal injection of monocrotaline (MCT) at 60 mg/kg. Human pulmonary artery smooth muscle cells (HPASMCs) were treated with platelet-derived growth factor BB (PDGF-BB) 20 ng/mL to construct PAH cell model in vitro. The results showed that in vivo studies, MCT could induce right ventricular wall hyperplasia, narrow the small and medium pulmonary artery cavity, up-regulate the expression of proliferating and migration-related proteins proliferating cell nuclear antigen (PCNA) and osteopontin (OPN), and down-regulate the expression of alpha-smooth muscle actin (α -SMA). Que reversed the MCT-induced results. This process works by down-regulating the transforming growth factor- β 1 (TGF- β 1)/ Smad2/3 signaling pathway. In vitro studies, Que had the same effect on PDGF-BB-induced proliferation and migration cell models.

Conclusions Que inhibits the proliferation, migration and phenotypic transformation of HPASMCs by down-regulating TGF- β 1/Smad2/Smad3 pathway, thereby reducing right ventricular hyperplasia (RVH) and pulmonary vascular remodeling, providing potential pharmacological and molecular explanations for the treatment of PAH.

Highlights

- (1) Que can significantly improve the hemodynamic changes, RVH and pulmonary vascular remodeling in MCT induced PAH rats.
- (2) Que inhibits the proliferation, migration and phenotypic transformation of HPASMCs by regulating TGF- β 1/Smad2/Smad3 pathway, thus playing a protective role in PAH pulmonary vascular remodeling.

Keywords Que, PAH, Proliferation, Migration, TGF- β 1

*Correspondence:

Ai-Mei Zhang

147460607@qq.com

Jun-Qiang Si

sijunqiang@shzu.edu.cn

Full list of author information is available at the end of the article



© The Author(s) 2024. **Open Access** This article is licensed under a Creative Commons Attribution-NonCommercial-NoDerivatives 4.0 International License, which permits any non-commercial use, sharing, distribution and reproduction in any medium or format, as long as you give appropriate credit to the original author(s) and the source, provide a link to the Creative Commons licence, and indicate if you modified the licensed material. You do not have permission under this licence to share adapted material derived from this article or parts of it. The images or other third party material in this article are included in the article's Creative Commons licence, unless indicated otherwise in a credit line to the material. If material is not included in the article's Creative Commons licence and your intended use is not permitted by statutory regulation or exceeds the permitted use, you will need to obtain permission directly from the copyright holder. To view a copy of this licence, visit <http://creativecommons.org/licenses/by-nc-nd/4.0/>.

Introduction

Pulmonary artery hypertension (PAH) is a rare multifactorial disease characterized by a progressive increase of pulmonary artery pressure, which eventually leads to right ventricular (RV) failure and death [1]. The pathogenesis of PAH is affected by many factors, including increased vascular resistance caused by pulmonary vasoconstriction, pulmonary vascular remodeling, and in situ thrombosis [2]. Phenotypic transformation, proliferation, and migration of smooth muscle cells are critical events of pulmonary vascular remodeling and participate in the occurrence and development of PAH [3]. As the signature proteins of cell proliferation and migration, proliferating cell nuclear antigen (PCNA) and osteopontin (OPN) are closely related to the process of cell proliferation and migration [4–6], and it is well known that they play a key role in vascular remodeling. In addition, when stimulated by various factors, pulmonary artery smooth muscle cells (PASMCs) transformed from a resting contractile phenotype to a proliferative synthetic phenotype, and the expression of alpha-Smooth Muscle Actin (α -SMA) protein representing the contractile phenotype was down-regulated, resulting in cell hyperplasia, hypertrophy, and media hypertrophy [7]. The proliferation and migration of PASMCs lead to arteriolarization of pulmonary arteries and increased expression of proliferative protein PCNA and migration protein OPN. Moreover, the proliferation of PASMCs promotes the synthesis of extracellular matrix and leads to changes in vascular remodeling. Thus, inhibition of the proliferation and migration of PASMCs and alleviating pulmonary vascular remodeling are of great significance for improving the development of PAH [8].

In recent years, with the research and development of traditional Chinese medicine, a new drug idea has been provided for disease treatment. Quercetin (3,3',4',5,6-pentahydroxyflavone, Que), as one of the most widely distributed natural flavonol compounds, is one of the six subclasses of flavonoid compounds and widely distributed in the root, stem, and fruit of many plants [9]. At present, Que exhibits a range of biological activities, including anti-oxidation, anti-tumor, anti-inflammatory, inhibition of fibrosis, cell proliferation and migration, and promotion of apoptosis [10–12]. Studies have demonstrated that Que can attenuate the progression of PAH by improving pulmonary vascular remodeling [13]. However, further investigation is needed to elucidate the underlying mechanisms involved in the protective role of Que.

Transforming growth factor- β 1 (TGF- β 1), as a classical signal pathway, forms heterotrimeric complexes with cell surface receptors. This interaction initiates the activation and phosphorylation of downstream Smad2 and Smad3 proteins. Subsequently, these phosphorylated

Smads form trimeric complexes with the nuclear protein Smad4, which translocates the signaling information from the plasma membrane to the nucleus. This process affects other transcription factors and ultimately regulates the expression of target genes [14, 15]. Studies indicate that TGF- β 1 promotes the proliferation and migration of HPASMCs by up-regulating Smad2/3 signaling pathway [15]. This upregulation leads to excessive extracellular matrix deposition, contributing to pulmonary vascular remodeling, increased pulmonary vascular resistance, and the development of PAH [16]. Therefore, targeting the TGF- β 1-Smad2/3 signaling pathway with specific drugs may become a promising therapeutic approach for the treatment of PAH.

Thus, this study aims to clarify the impact of Que on the proliferation, migration and phenotype transformation of HPASMCs and its potential mechanisms, to provide a new theoretical basis for the treatment of PAH.

Material and methods

Animal model and treatment plan

A total of 24 male Sprague-Dawley (SD) rats (8–10 w; 200–250 g) were purchased from Vitong Lever [Animal Certificate No.: SCXK (Beijing) 2012-0001]. The rats were randomly divided into four groups: CON group (blank control group, $n=6$); MCT group ($n=6$), where rats received intraperitoneal injections (i.p.) of MCT (60 mg/kg, Sigma-Aldrich, MO, United States) from the 1st day to the 28th day [13, 15]; MCT + Que group ($n=6$), where rats received MCT (60 mg/kg) intraperitoneally on day 1 and Que (100 mg/kg/d, Sigma-Aldrich, MO, USA) administered orally from day 15 to day 28; Que group ($n=6$), from the 15th day to the 28th day, Que (5 mg/kg/d) was administered continuously for 14 days [16, 17]. On day 28, echocardiographic measurements were performed on all animals. The rats were then euthanized under deep anesthesia (i.p. of 3% pentobarbital sodium, 100 mg/kg), and their heart and lung tissues were collected for further analysis [18].

Doppler echocardiography measurement

Doppler echocardiography was used to identify PAH on the 28th day of SD rats modeling. The Doppler echocardiography parameter "Pulmonary Artery Acceleration Time" (PAAT) is considered as an echocardiographic indicator of PAH [19], which is negatively correlated with the invasive measured mean pulmonary artery pressure (mPAP). Transthoracic echocardiography was performed using a Vivid E9 ultrasound system equipped with a 12-MHz transducer (GE Healthcare). The rats were anesthetized with an i.p. injection of 3% sodium pentobarbital (40 mg/kg). PAAT was measured near the pulmonary valve on the left chest. According to the current

guidelines of the American Society of Echocardiography, mPAP can be calculated according to the following formula: $mPAP = 72 - (0.42 \times PAAT)$, $PAAT < 120$ ms) [18, 20]. Following echocardiographic assessment, the rats were sacrificed under deep anesthesia (i.p. 3% pentobarbital sodium, 100 mg/kg) [20], and the lung and heart tissues were collected for analysis. Echocardiographic data were analyzed using Echopac BT11 software (v.6.5; GE Healthcare).

Right ventricular hypertrophy measurement

To evaluate the right ventricular hypertrophy index (RVHI), rats were sacrificed under deep anesthesia (i.p. 3% Pentobarbital Sodium, 100 mg / kg), and the heart tissue was collected and weighed. Atrium and external blood vessels were carefully removed from the isolated heart using 0.9% normal saline. The weights of both right ventricle (RV) and left ventricle (LV) plus septum (S) were recorded [13, 21]. The RVHI was calculated by $[RV / (LV + S)]$ [13, 22].

H&E staining

Lung tissues were harvested, fixed, dehydrated, transparent, waxed, embedded, sectioned, patched and cut into slices (4 μ m). The slides were stained with hematoxylin and eosin (HE) for morphometric analysis. The histopathological changes of pulmonary arterioles (15–50 μ m) and middle and small pulmonary arteries (50–150 μ m) were observed and photographed with an Olympus BX51 digital camera. Two professional pathologists randomly selected 20 different microscopic fields of each slide and analyzed pulmonary vascular remodeling with Image-Pro Plus v.6.0 (Media cybernetics, Inc.). Pulmonary vascular remodeling was evaluated by the percentage of the thickness of the vessel wall (WT%) and the percentage of the vessel wall area (WA%). $WT\% = [2 \times (\text{blood vessel outer diameter} - \text{blood vessel inner diameter})] / (\text{blood vessel outer diameter}) \times 100\%$; $WA\% = (\text{total area of blood vessel} - \text{blood vessel Internal area}) / \text{total area of blood vessel} \times 100\%$ [23].

Immunofluorescence analysis

For immunofluorescence analysis, paraffin sections of each group were dewaxed or cells were seeded on 6-well glass chamber slides, fixed and sealed with 4% paraformaldehyde. These sections or cells were then treated with 0.3% Triton and incubated overnight at 4 °C with anti PCNA (ab29, Abcam, Cambridge, UK; 1:200 dilution), anti OPN (ab8448, Abcam; 1:200 dilution), anti α -SMA (ab124964, Abcam; 1:100 dilution) and anti TGF- β 1 (ab179695, Abcam; 1:100 dilution) antibodies [4, 24–26]. Then incubated at 37 °C for 2 h with secondary antibody

(FITC labeled goat anti-rabbit IgG, Beijing Zhongshan Jinqiao Biotechnology, 1:100; TRITC labeled anti-mouse IgG, Beijing Zhongshan Jinqiao Biotechnology, 1:100). The nucleus was stained with DAPI at 37 °C for 30 min (1:1000, D9542, Sigma-Aldrich; MerckKGaA, USA). The stained slices and cells were observed under a confocal laser scanning microscope (LSM710, Carl Zeiss AG, Oberkochen, Germany).

Immunohistochemical staining

All immunohistochemical experiments were performed on paraffin-embedded slides (4 μ m). The primary antibodies anti α -SMA (ab124964, Abcam; 1:100 dilution) and anti TGF- β 1 (ab179695, Abcam; 1:100 dilution) were incubated overnight at 4 °C [27–29]. Then the slides were incubated for 2 h min with the appropriate secondary antibody at 37 °C. After reverse staining, dehydration, dewaxing, and sealing, observed and photographed under an inverted microscope (LSM710; Carl Zeiss AG, Oberkochen, Germany). Five blood vessels with a diameter of 50~150 μ m were randomly chosen from each slide to observe the distribution of staining of small and medium arteries in pulmonary tissue.

Cell culture and treatment

HPASMCs (Shanghai Cybertron Biotechnology Co., Ltd., China) were cultured in DMEM high glucose medium (Gibco) supplemented with 10% fetal bovine serum and 1% penicillin-streptomycin (Gibco). The cells were Incubated at 37 °C in a humidified 5% CO₂ atmosphere.

CON group cells received no drug intervention. Cells in PDGF-BB group were treated with PDGF-BB (20 μ mol/ml, 10014B, Pepro Tech, US) for 24 h. In PDGF-BB + Que group, Que (60 μ mol/ml, Q4951, Sigma-Aldrich; Merck-KGaA) was pretreated for 2 h [30] and then treated with PDGF-BB (20 μ mol/ml) for 24 h [31]. Que group cells were treated with Que (60 μ mol/ml) for 2 h.

CCK-8 proliferation assay

The effect of different concentrations (0,2.5,5,10,20,40,80 ng/mL) of PDGF-BB on HPASMCs proliferation was assessed by CCK-8. Briefly, HPASMCs (10⁵ cells /ml) were seeded into 96-well plates and cultured at 37 °C in a humidified 5% CO₂ atmosphere. Then incubated with different concentrations of PDGF-BB for 24 h [31, 32]. CCK-8 solution was added and incubated in the dark for 1 h, and then they were tested by a microplate absorbance reader at 450 nm.

Furthermore, to detect the effect of Que on cell proliferation, different concentrations (0, 15, 30, 60, 90, 120 μ mol/mL) of Que [13, 17, 33] were added 96-well plate cells that had been incubated with 20 ng/ml PDGF-BB for 24 h. CCK-8 solution was added and incubated in the

dark for 1 h, and then they were tested by a microplate absorbance reader at 450 nm.

EdU incorporation assay

The EdU incorporation assay was performed according to the manufacturer's instructions (K1075, APEX BIO, US). HPASMCs were seeded into 6-well plates and cultured at 37 °C in a humidified 5% CO₂ atmosphere. Following drug treatments, cells from each group were incubated with EdU component A for 2 h. The cells were then trypsinized, centrifuged, fixed, permeabilized, and washed. The reaction solution was added into a centrifuge tube and incubated in darkness at room temperature for 30 min. After centrifugation and washing, the EdU proliferation was analyzed by flow cytometry. The proliferation ability of HPASMCs was reflected by its proliferation ratio [15, 34].

Cell scratch test

HPASMCs in the logarithmic growth phase were inoculated into 6-well plates with 5 horizontal lines drawn at equal intervals on the back, and cultivated at 37 °C and 5% CO₂ until the cell density reached 80%. Five cell-free bands were generated in each well uniformly using a 1 mL pipet tip. Washed twice with PBS and then incubated with 1 mL DMEM / H serum-free medium, treated with different drugs. Images were recorded and assessed at 0 h and 24 h using Olympus inverted microscope. And the migration distance was estimated using ImageJ software (NIH, MD, USA). The cell migration rate (%) = [(Average area of scratches at 0 h—Average area of scratches at 24 h)/Average area of scratches at 0 h] × 100% [35, 36].

Transwell™ test

Inoculated 200 μL of cell suspension (cell density of 10⁵ cells /mL) in the upper chamber. 600 μL DMEM/H complete medium containing 10% FBS was added to the lower chamber, and cultured at 37 °C in a humidified atmosphere with 5% CO₂. Different drugs were added for intervene after the cells adhered to the wall. After 24 h, the cells below the sieve membrane were then fixed with 4% paraformaldehyde and stained with 0.1% crystal violet. A cotton swab was used to wipe the cells on the upper surface of the chamber gently. Five different visual fields were randomly selected, the cells that invaded the submembrane surface were counted [34, 37].

Western blot analysis

For western blotting, after protein electrophoresis in each group, after separation with 10% SDS-PAGE, the target protein was transferred to PVDF membrane and blocked with 5% skim milk for 2 h. Proteins were incubated overnight at 4 °C with the following antibodies: anti- GAPDH (ab8245, Abcam, Cambridge,

UK; 1:10,000), anti-PCNA (ab29, Abcam; 1:1000), anti-OPN (ab8448, Abcam; 1:700), anti- α-SMA (ab124964, Abcam; 1:1000), anti-TGF-β1 antibody (ab179695, Abcam; 1:100), anti-Smad2 (ab40855, Abcam; 1:1000), anti-Smad3 (ab40854, Abcam; 1:1000), anti-p Smad2(ab188334, Abcam; 1:1000) and anti-p smad3(ab52903, Abcam;1:1000) [15, 38, 39]. Horseradish peroxidase-labeled anti-mouse antibody or anti-rabbit antibody (Beijing Zhongshan Jinqiao Biotechnology; 1:1000) was used as the secondary antibody incubated at room temperature for 2 h. The membranes were visualized with enhanced chemiluminescence reagent (Thermo Science, Waltham, MA, USA) and Image J software (Bethesda, USA, National Institutes of Health) were used to quantize the grayscale values. Protein levels were normalized to GAPDH.

Quantitative RT-PCR

RNA was isolated using Trizol (Thermo Science, Waltham, MA, USA) following the manufacturer's instructions. And cDNA was synthesized using qRT-PCR kit (Thermo science, Waltham, Ma, USA). The target genes PCNA, OPN, α-SMA, TGF-β1, Smad2, Smad3 and GAPDH were amplified by RT-PCR using cDNA as template. The reaction temperature was 95 °C, the pre denaturation time was 2 min, the reaction temperature was 95 °C for 5 s, the reaction temperature was 60 °C for 10 s, a total of 40 cycles. The amplified primer sequences are as follows:

PCNA	CCTGCTGGGATATTA GCTCCA	CAGCGGTAGGTGTCG AAGC
OPN	AAGTTTCGACACCT GACAT	GTATGCACCACTCAACTC CTCG
α-SMA	CTATGAGGGCTATGC CTTGCC	GCTCAGCAGTAGTAA CGAAGGA
TGF-β1	CAATTCCTGGCGATA CCTCAG	GCACAACTCCGGTGA CATCAA
Smad2	CCGACACACCGAGAT CCTAAC	GAGGTGGCGTTTCTG GAATATAA
Smad3	TGGACGCAGGTTCTC CAAA	CCCGGCTCGCAGTAG GTAAC
GAPDH	GGAGCGAGATCCCTC CAAAAT	GGCTGTTGTCATACTTCT CATGG

The mRNA level of GAPDH was used as a control, and ran a standard curve to determine the relative level of each target gene. The relative gene expression level was calculated by 2-ΔΔCt method. For each experimental condition, all PCR were repeated at least three times [40, 41].

Statistical analysis

Statistical software SPSS 20.0 and GraphPad Prism 8.0 were used to analyze the experimental results. All

results were expressed as mean±SD. Statistical comparisons between two groups were made by the two-way ANOVA. Probability values <5% ($P < 0.05$) were considered significant.

Results

Que inhibits pulmonary hemodynamic changes and RVH in PAH rats

The echocardiogram of pulmonary artery blood was detected by the Doppler ultrasonic diagnostic instrument. Compared to the control group ($n=6$) (Fig. 1A), the MCT group showed a mid systolic notch, a forward shift in the peak, and a significant reduction in PAAT value decreased ($P < 0.01$, $n=6$) (Fig. 1C). And mPAP

significantly increased ($P < 0.01$, $n=6$) (Fig. 1D), with mPAP values exceeding 50 mmHg (Fig. 1D). Compared to the CON group, HE results of heart cross-section showed significant hypertrophy of the RV heart in the MCT group ($n=6$) (Fig. 1B), and significantly increased RVHI% ($P < 0.01$, $n=6$) (Fig. 1E). These results indicate that our animal model of PAH has been successfully prepared.

Compared to MCT group, the MCT+Que group showed a significant increase in PAAT ($P < 0.01$, $n=6$) (Fig. 1C), and a significant decrease in the mPAP ($P < 0.01$, $n=6$) (Fig. 1D) and RVHI% ($P < 0.05$, $n=6$) (Fig. 1E). By contrast, the RVH of the MCT+Que group was lower than that of the MCT group (Fig. 1B). There

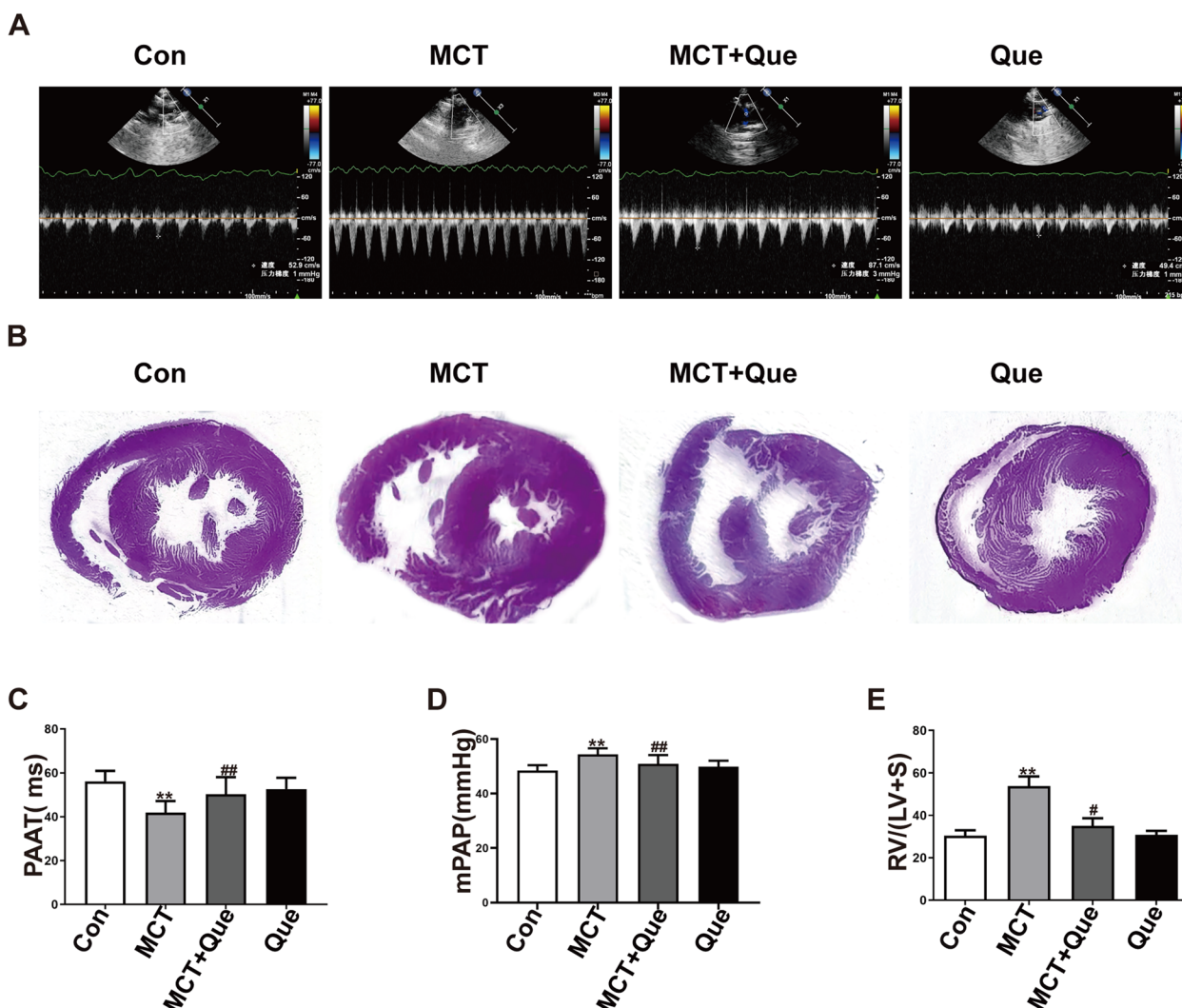


Fig. 1 Que improves hemodynamics and right ventricular remodeling in PAH rats. **A** The pulmonary haemodynamic spectrum; **B** Cardiac cross-sectional HE results; **C** The comparison of PAAT; **D** The comparison of mPAP; **E** The comparison of RVHI%. MCT vs CON, ** $P < 0.01$; MCT+Que vs MCT, # $P < 0.05$, ## $P < 0.01$. ($n=6$)

was no significant difference between Que group and CON group. HE staining was used to observe the structural differences of the small pulmonary arterioles (15–50 μm) ($n=6$) (Fig. 2A) and medium sized pulmonary

arteries (50–150 μm) in each group ($n=6$) (Fig. 2B). We found that the pulmonary artery cells in CON group were evenly distributed, continuous and structurally intact; while the pulmonary artery cells in the MCT

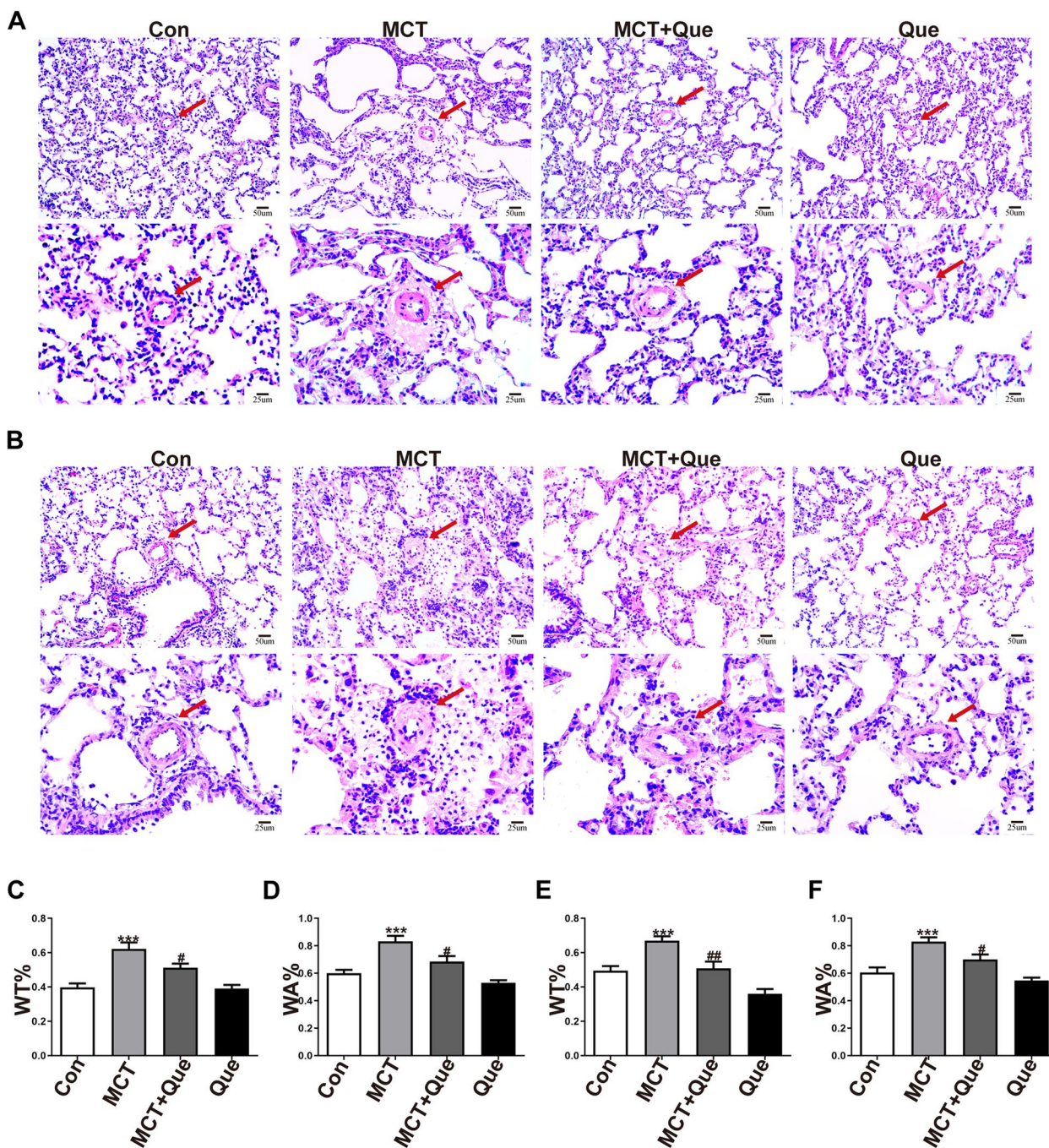


Fig. 2 Que improves pulmonary artery remodeling in PAH rats. **A** HE staining of lung tissue and pulmonary small artery at $\times 200$ and $\times 400$; **B** He staining of lung tissue and medium pulmonary artery at $\times 200$ and $\times 400$; **C** The statistical analysis of the small pulmonary artery's WT%; **D** The statistical analysis of the small pulmonary artery's WA%; **E** The statistical analysis of the medium pulmonary artery's WT%; **F** The statistical analysis of the medium pulmonary artery's WA%. The arrow points to the pulmonary artery. MCT vs CON, *** $P < 0.001$; MCT + Que vs MCT, # $P < 0.05$, ## $P < 0.01$. ($n=6$)

group were arranged disorderly, the area of the lumen was reduced, deposition of exogenous matrix, and the thickness of the tube wall was significantly increased. MCT administration induced significant enhancement of WT% (Fig. 2E) and WA% (Fig. 2F) of medium sized pulmonary arteries ($P < 0.001$, $n = 6$). Meanwhile, Que treatment rescued this MCT-promoted WT% ($P < 0.01$, $n = 6$) and WA% ($P < 0.05$, $n = 6$) increase. The results showed that Que effectively improved the vascular remodeling of pulmonary artery. The changes of WT% ($P < 0.05$, $n = 6$) (Fig. 2C) and WA% ($P < 0.05$, $n = 6$) (Fig. 2D) of the pulmonary arterioles had a same trend with those of the medium sized pulmonary arteries.

Effect of Que on PCNA, OPN and α -sma protein expression in pulmonary blood vessels and lung tissues of PAH rats

Immunohistochemistry and immunofluorescence were used to detect the expression changes of PCNA, OPN and α -SMA in rat lung tissue (Fig. 3A, B). Semi-quantitative fluorescence results showed that after labeled with specific vascular marker protein α -SMA, the expression of α -SMA protein in blood vessels of CON groups was significantly higher, while the expression intensity of α -SMA protein in blood vessels of MCT group was decreased, and the fluorescence intensity of PCNA and OPN protein in blood vessels and lung tissues was increased ($n = 3$) (Fig. 3A, B). After Que intragastric treatment, compared with MCT group, α -SMA expression was up-regulated, while PCNA and OPN protein expression was down-regulated ($n = 3$) (Fig. 3A, B). The trend of SMA protein expression in immunohistochemistry was consistent with the results of semi-quantitative fluorescence ($n = 3$) (Fig. 3C).

Western blot was used to further detect OPN, PCNA and α -SMA protein levels in the tissue homogenate of rat pulmonary blood vessels ($n = 6$) (Fig. 3D). Compared with CON group, the protein expression levels of PCNA ($P < 0.001$, $n = 6$) (Fig. 3E) and OPN ($P < 0.001$, $n = 6$) (Fig. 3F) in the MCT group increased significantly, and there was a significantly decrease in the expression level of α -SMA protein ($P < 0.01$, $n = 6$) (Fig. 3G). Compared with MCT group, MCT+Que group showed decreases in the expression of PCNA ($P < 0.05$, $n = 6$) (Fig. 3E) and OPN ($P < 0.01$, $n = 6$) (Fig. 3F), but an increase in the expression of α -SMA ($P < 0.05$, $n = 6$) (Fig. 3G).

Que inhibits TGF- β 1-Smad2/3 signaling pathway in pulmonary vessels of PAH rats

To investigate the changes of TGF- β 1-Smad2/3 signaling pathway in pulmonary vessels of MCT-induced PAH rats and whether Que plays a role in this process. The expression of TGF- β 1 protein in rat lung tissue and pulmonary vessels was analyzed by immunohistochemistry and

western blot (Fig. 4A, B). Compared with CON group, narrowing of the pulmonary artery lumen and thickening of the vessel walls were observed in MCT group, and the expression level of TGF- β 1 increased ($n = 3$) (Fig. 4A). After Que treatment, there was a reduction in the thickening degree of vessel walls, and the expression of TGF- β 1 in pulmonary vessels and lung tissues was significantly decreased ($n = 3$) (Fig. 4A).

Western blot was used to further detect the expression of TGF- β 1-Smad2/3 pathway proteins ($n = 6$) (Fig. 4B) in rat pulmonary artery. MCT administration induced significant increases in the pulmonary vascular TGF- β 1 ($P < 0.01$, $n = 6$) (Fig. 4C), p-Smad2 and p-Smad3 ($P < 0.05$, $n = 6$) (Fig. 4D-E). Meanwhile, the expressions of TGF- β 1 ($P < 0.05$, $n = 6$) (Fig. 4C), p-Smad2 and p-Smad3 ($P < 0.05$, $n = 6$) (Fig. 4D-E) in MCT + Que group were significantly reduced.

Effect of Que on the vitality of HPASMCs induced by platelet derived PDGF-BB in vitro

As shown in supplementary Figs. 1 and 2, PDGF-BB and Que are not cytotoxic to HPASMCs and can induce cell proliferation in a concentration-dependent manner. When the concentration of PDGF-BB reached 20 ng/ml, the effect on cell proliferation was most obvious ($P < 0.001$, $n = 6$) (Supplementary Fig. 1B). Therefore, in this study, 20 ng/ml PDGF-BB treatment was selected. The effect was most statistically significant when Que reached 60 μ mol/ml ($P < 0.001$, $n = 6$) (supplementary Fig. 2B). Therefore, 60 μ mol/ml was selected as the intervention concentration of Que in this study.

Effects of Que on proliferation, migration and phenotypic transformation of HPASMCs induced by PDGF-BB in vitro

EdU assay was used to investigate the role of Que in the proliferation ability of HPASMCs in vitro (Fig. 5A). The results showed that PDGF-BB treatment could significantly increase HPASMCs proliferation ($P < 0.01$, $n = 3$) (Fig. 5D). There was a reduction in the cell proliferation rate of PDGF-BB + Que group ($P < 0.05$, $n = 3$) (Fig. 5D).

Cell migration was analyzed by cell scratch test and TranswellTM chamber test. Wound closure levels ($P < 0.01$, $n = 6$) (Fig. 5E) and the migration number of HPASMCs ($P < 0.01$, $n = 6$) (Fig. 5F) were increased significantly after PDGF-BB stimulation for 24 h. Que treatment decreased wound closure levels ($P < 0.01$, $n = 6$) (Fig. 5E) and the migration number of HPASMCs ($P < 0.01$, $n = 6$) (Fig. 5F) in PDGF-BB + Que group, suggesting that the PDGF-BB-induced migration was inhibited by Que.

In addition, the expression of PCNA, OPN, α -SMA proteins indicated the level of cell proliferation, migration and phenotypic transformation. As shown in Fig. 6 (Fig. 6A-C), PCNA was mainly expressed in nucleus,

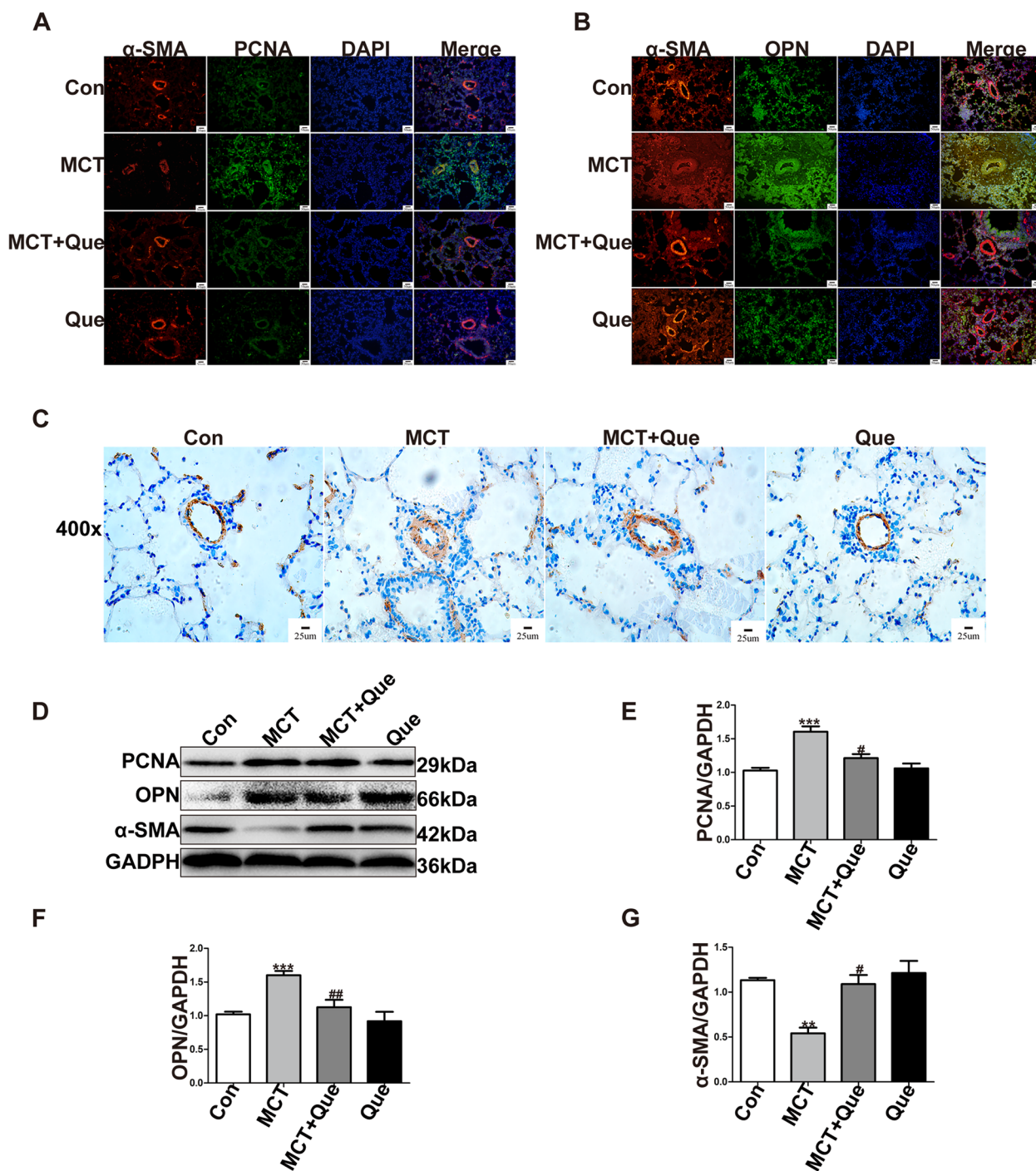


Fig. 3 Effects of Que on the distribution and expression of PCNA, OPN, α-SMA in pulmonary blood vessels of MCT-induced PAH rats. **A** Immunofluorescence of α-SMA and PCNA at ×200; **B** Immunofluorescence of α-SMA and OPN at ×200; **C** Immunohistochemical expression of α-SMA at ×400; **D** Western blotting of PCNA, OPN, α-SMA and GAPDH; **E** Analysis of relative expression of PCNA by Western blot; **F** Analysis of relative expression of OPN by Western blot; **G** Analysis of relative expression of α-SMA by Western blot. MCT vs CON, ** $P < 0.01$, *** $P < 0.001$; MCT+Que vs MCT, # $P < 0.05$, ## $P < 0.01$. ($n = 3$ to 6)

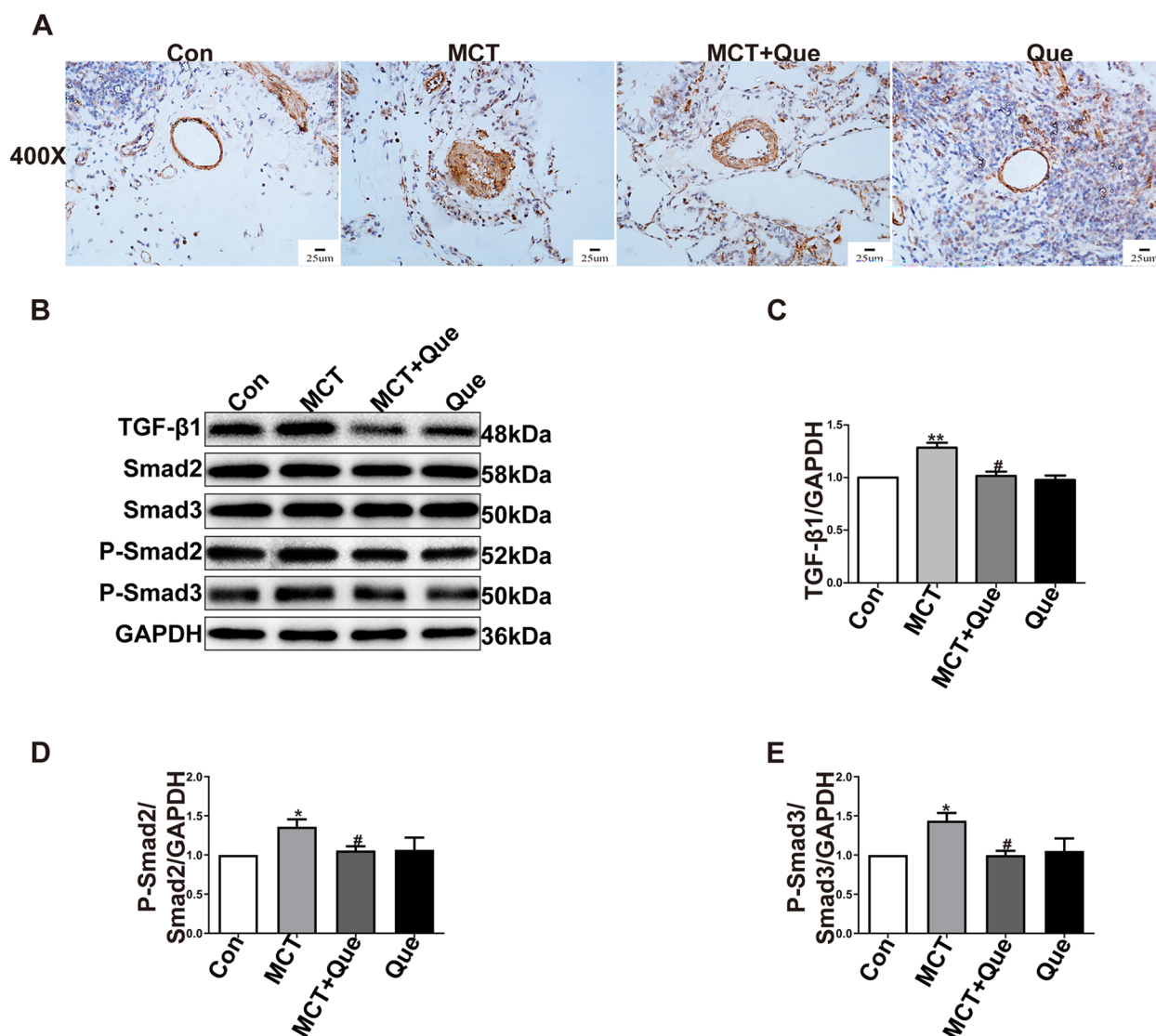


Fig. 4 Effects of Que on the distribution and expression of TGF- β 1-Smad2/3 signal pathway in pulmonary blood vessels of MCT-induced PAH rats. **A** Immunohistochemical expression of TGF- β 1 at $\times 400$; **B** Western blotting of TGF- β 1, Smad2/3, p-Smad2/3 and GAPDH; **C** Analysis of relative expression of TGF- β 1 by Western blot; **D** Analysis of relative expression of p-Smad2/ Smad2 by Western blot; **E** Analysis of relative expression of p-Smad3/ Smad3 by Western blot. MCT vs CON, * $P < 0.05$, ** $P < 0.01$; MCT+Que vs MCT, # $P < 0.05$. ($n = 3$ to 6)

but also in cell membrane and cytoplasm; OPN was expressed in cell membrane, nucleus and cytoplasm; α -SMA is mainly expressed in cytoplasm. After PDGF-BB intervention, the expression intensity of PCNA and OPN protein increased and the expression of α -SMA protein decreased in HPASMCs ($n = 3$) (Fig. 6A-C). Que pretreatment reduced the expression intensity of PCNA and OPN protein, but increased the expression of α -SMA protein ($n = 3$) (Fig. 6A-C).

Similarly, Western blot and qRT-PCR results were consistent with semi-quantitative immunofluorescence results,

both at the protein level and at the mRNA level ($n = 3$) (Fig. 6D-J). PDGF-BB could significantly increase the protein and mRNA expressions of PCNA ($P < 0.01$, $n = 6$) (Fig. 6E, H) and OPN ($P < 0.01$, $n = 6$) (Fig. 6F, I), decrease the and mRNA expressions of α -SMA ($P < 0.001$, $P < 0.01$, $n = 6$) (Fig. 6G, J). After Que pretreatment, PDGF-BB + Que group showed decreases in the protein and mRNA expressions of PCNA ($P < 0.01$, $P < 0.05$, $n = 6$) (Fig. 6E, H) and OPN ($P < 0.05$, $P < 0.01$, $n = 6$) (Fig. 6F, I), and a significant increase in α -SMA protein and mRNA expressions ($P < 0.01$, $P < 0.05$, $n = 6$) (Fig. 6G, J). There was no significant difference between Que group and CON group.

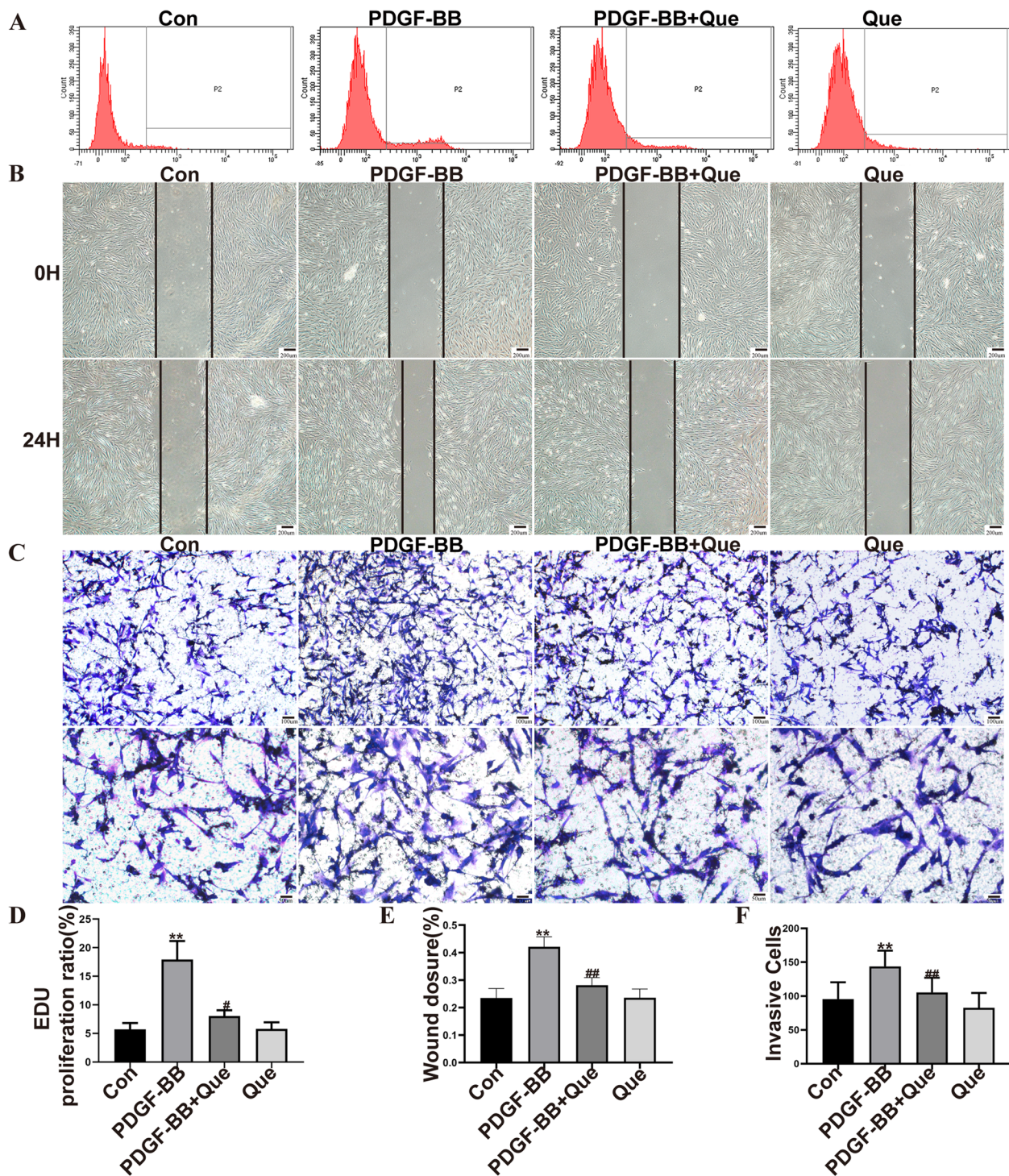


Fig. 5 Effect of Que on proliferation, migration and phenotypic transformation of HPASMCs induced by PDGF-BB in vitro. **A** HPASMCs proliferation was detected by flow cytometry (EDU); **B** The migration ability of HPASMCs was tested by scratch test at $\times 50$; **C** Transwell™ cell crystal violet staining was used to detect the migration of HPASMCs at $\times 100$ and $\times 200$; **D** HPASMCs proliferation rate was analyzed by flow cytometry (EDU); **E** The migration ratio of scratch was quantitatively analyzed; **F** Cell invasion relative quantitative analysis of migration ratio. PDGF-BB vs CON, ** $P < 0.01$; PDGF-BB + Que vs PDGF-BB, # $P < 0.05$, ## $P < 0.01$. ($n = 3$ to 6)

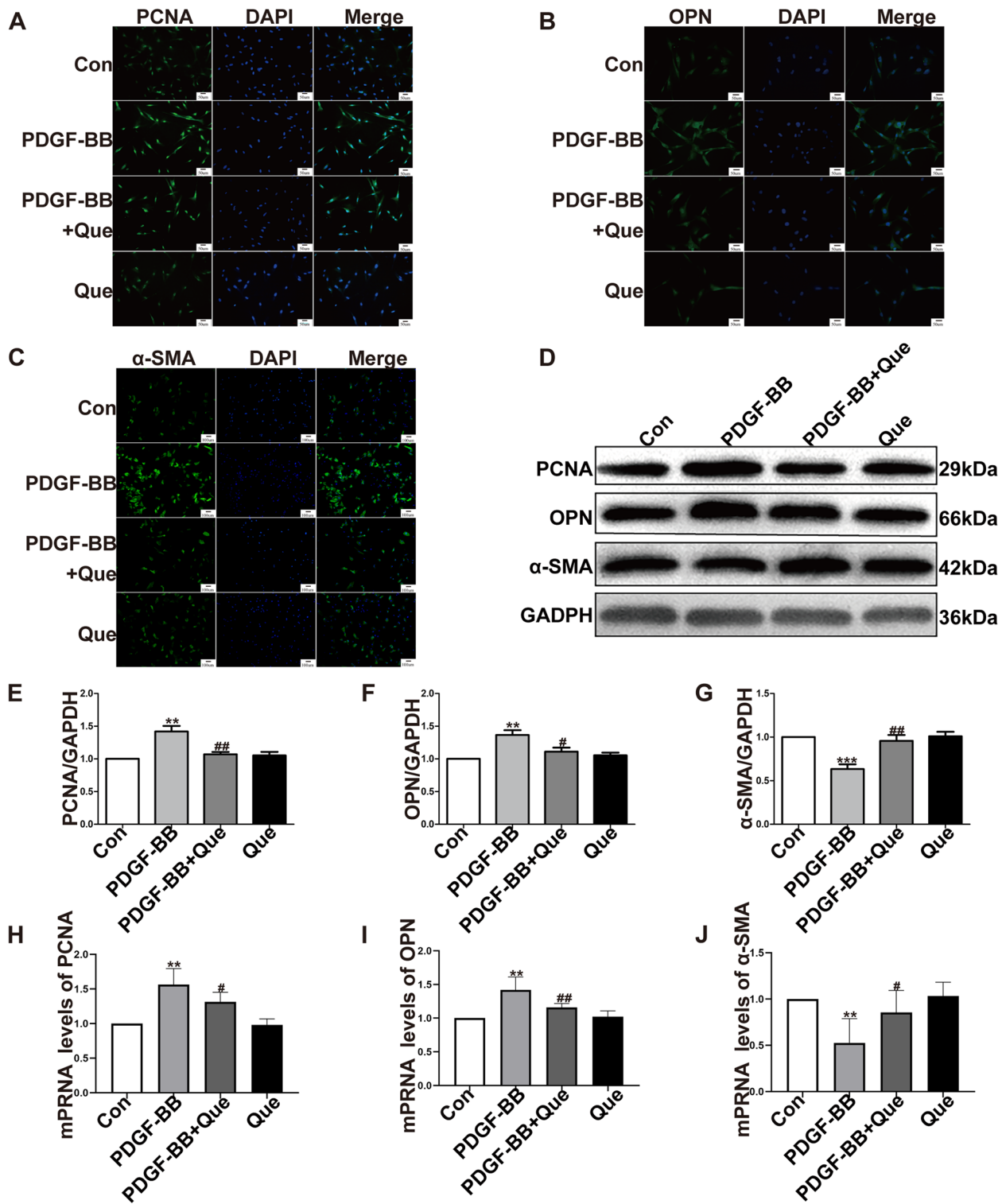


Fig. 6 Effects of Que on PCNA, OPN and α-SMA distribution and expression in PDGF-BB induced HPASMCs. **A** Immunofluorescence of PCNA of HPASMCs at × 200; **B** Immunofluorescence of OPN of HPASMCs × 200; **C** Immunofluorescence of α-SMA of HPASMCs at × 200; **D** Western blotting of PCNA, OPN, α-SMA and GAPDH of HPASMCs; **E** Analysis of relative expression of PCNA by Western blot; **F** Analysis of relative expression of OPN by Western blot; **G** Analysis of relative expression of α-SMA by Western blot; **H** Analysis of relative expression of mRNA levels of PCNA; **I** Analysis of relative expression of mRNA levels of OPN; **J** Analysis of relative expression of mRNA levels of α-SMA. PDGF-BB vs CON. ** $P < 0.01$, *** $P < 0.001$; PDGF-BB+Que vs PDGF-BB, # $P < 0.05$, ## $P < 0.01$. ($n = 3$ to 6)

Effect of Que on TGF- β 1/Smad2/Smad3 signaling pathway in HPASMCs induced by PDGF-BB in vitro

To explore the potential molecular mechanisms, we assessed the changes of TGF- β 1/Smad2/3 signaling pathway. Immunofluorescence and western blot were used to detect the expression of TGF- β 1 in HPASMCs (Fig. 7A-B). Figure 7A showed that Que intervention could reverse the elevated levels of TGF- β 1 caused by PDGF-BB ($n=3$). Western blot showed that TGF- β 1 ($P<0.01$, $n=6$) (Fig. 7C), p-Smad2 and p-Smad3 ($P<0.01$, $n=6$) (Fig. 7D-E) proteins in PDGF-BB group were significantly enhanced compared with CON group. In PDGF-BB+Que group, there were significant decreases in the expressions of TGF- β 1 ($P<0.01$, $n=6$) (Fig. 7C), p-Smad2 and p-Smad3 ($P<0.05$ or $P<0.01$, $n=6$) (Fig. 7D-E), but no significant changes were observed in the expression of total Smad2/3 proteins ($n=6$) (Fig. 7B).

Furthermore, we used qRT-PCR to detect the mRNA levels of TGF- β 1 and Smad2/3 in HPASMCs (Fig. 7F-H). Interestingly, although TGF- β 1 mRNA expression levels in all groups were consistent with Western blot results (Fig. 7F), there was no significant effect on Smad2/3 mRNA expression in all groups (Fig. 7G-H).

Discussion

The two main findings of this study are as follows: (1) Que can significantly improve the hemodynamic changes, RVH and pulmonary vascular remodeling in MCT induced PAH rats; (2) Que inhibits the proliferation, migration and phenotypic transformation of HPASMCs by regulating TGF- β 1/Smad2/Smad3 pathway, thus playing a protective role in PAH pulmonary vascular remodeling.

PAH is a rare progressive disease characterized by pulmonary vascular remodeling due to the progressive increase of the average pulmonary artery pressure, and ultimately leads to right heart failure and death [3].

Que, as one of the flavonol compounds existing in many plants, has a variety of beneficial effects [9–11]. Studies have shown that Que can stimulate melanoma cell migration and invasion [42]. A variety of signaling molecules involved in cell survival, proliferation, migration and adhesion regulated by Que to reduce the migration ability of ovarian cancer cells [43], as well as to inhibit the proliferation and migration of various cancer cells to achieve the therapeutic effects. Additionally, Que exhibits pharmacological protective effects in cardiovascular diseases in the process of vascular dilation [43–45]. Some studies have indicated that Que has a protective effect on PAH rats, but its precise mechanism underlying this effect remain unclear. In vivo, we observed that administered Que for 14 days following MCT injection led to an increase in PAAT and a decrease in mPAP, indicating that

Que could effectively reduce pulmonary artery wall pressure. Additionally, Que treatment decreased right ventricular thickness, reduced the wall thickness and lumen area of medium-sized pulmonary arteries, and increased the vascular lumen space. The above results indicate that Que can effectively inhibit the mean pulmonary artery pressure, RVH and pulmonary arteriole remodeling in MCT induced PAH rats.

Pulmonary vascular remodeling is a crucial pathophysiological change of PAH, in which the proliferation, migration and phenotypic transformation of PSMCs in the vascular media is one of the key events of pulmonary vascular remodeling. As a potent mitogen, PDGF-BB stimulates proliferation and migration in various cell types, including PSMCs. In addition, PDGF-BB enhances the number of mitochondria and expands the endoplasmic reticulum in PSMCs, leading to a shift from contractile to synthetic phenotypes and an increase in collagen content [5, 31, 35]. Due to the strong toxic effects of MCT on cells, we used PDGF-BB to stimulate excessive proliferation and migration of HPASMCs as an alternative approach to model PAH in vitro. In the current study, after the intervention of Que, the proliferation, scratch healing and migration of HPASMCs were significantly inhibited, suggesting that Que has a protective effect on PAH induced pulmonary vascular remodeling by inhibiting the proliferation and migration of HPASMCs.

According to research, pulmonary vessels have strong plasticity. When the vessels are stimulated by pathophysiology such as inflammatory factors, ischemia, hypoxia, dust, and NO, the cell phenotype changes from a highly differentiated contraction phenotype to a poorly differentiated synthetic phenotype, such as the expression of α -SMA and SM22a proteins decreases, and the expression of OPN and ephrin proteins increases [6, 7]. This has been fully verified both in vivo and in vitro. Quercetin can well inhibit the expression of OPN and increase the expression of α -SMA in PAH lung vessels and cells by immunohistochemistry, immunofluorescence and Western Blot, which further indicates that Que has a strong inhibitory effect on phenotypic transformation by transforming cells from contractile type to synthetic type. To some extent, the pulmonary vascular remodeling was reversed. As a key protein of abnormal cell proliferation, PCNA is related to cell DNA synthesis and is an important indicator of cell proliferation. In addition to being a marker protein of phenotypic transformation, OPN is also a recognized key protein representing migration, which affects cell migration and cytoskeleton protein metabolism in extracellular matrix. Changes in a variety of cancer cells and smooth muscle cells indicate changes in cell migration ability [4, 6, 46]. Therefore, in this study,

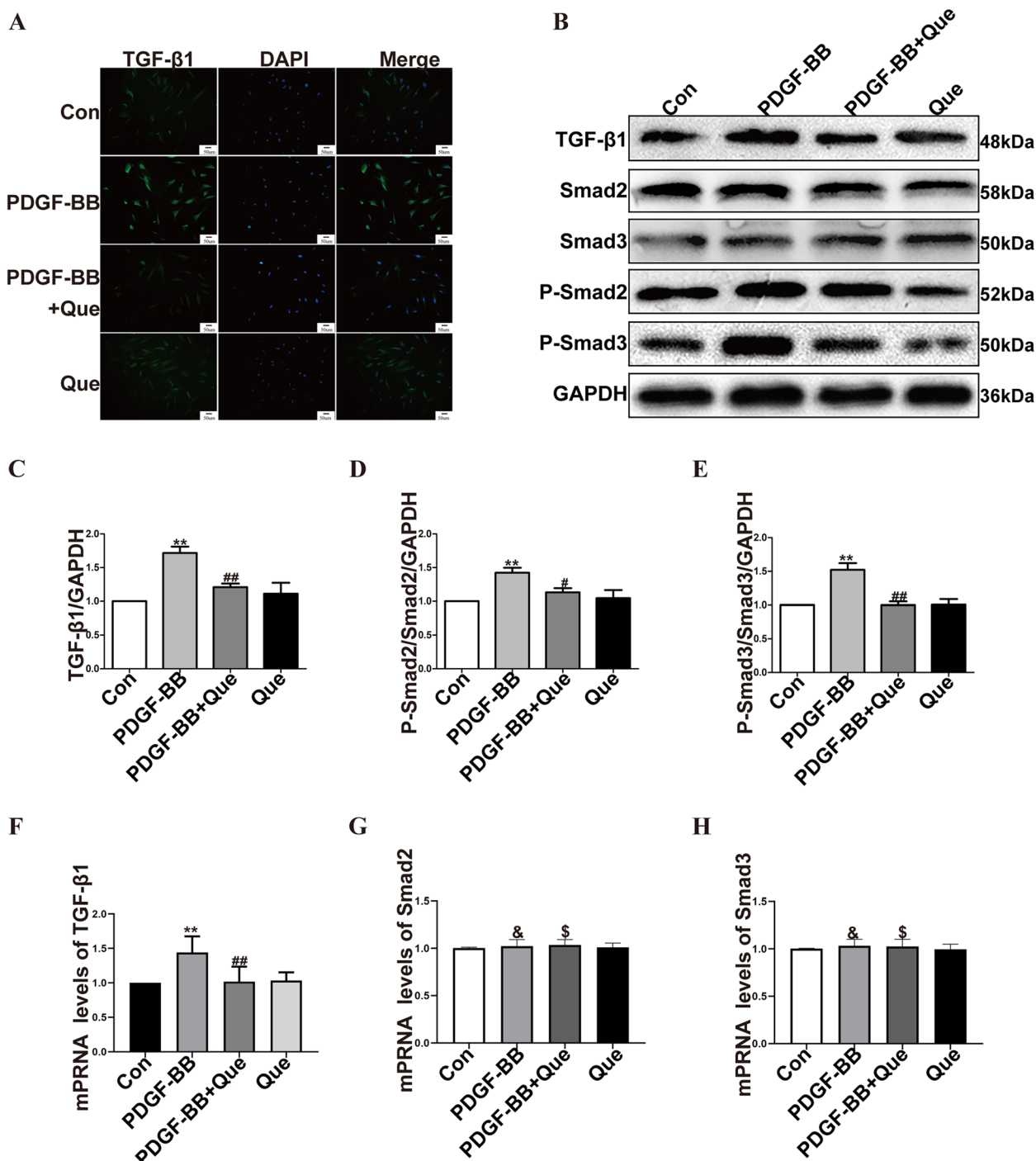


Fig. 7 Effects of Que on TGF-β1-Smad2/3 signal pathway distribution and expression in PDGF-BB induced HPASMCs. **A** Immunofluorescence of TGF-β1 of HPASMCs at ×200; **B** Western blotting of TGF-β1, Smad2/3, p-Smad2/3 and GAPDH of HPASMCs; **C** Analysis of relative expression of TGF-β1 by Western blot; **D** Analysis of relative expression of p-smad3/Smad2 by Western blot; **E** Analysis of relative expression of p-smad3/Smad3 by Western blot; **F** Analysis of relative expression of mRNA levels of TGF-β1; **G** Analysis of relative expression of mRNA levels of Smad2; **H** Analysis of relative expression of mRNA levels of Smad3. PDGF-BB vs CON, ** $P < 0.01$, & $P > 0.05$; PDGF-BB + Que vs PDGF-BB, # $P < 0.05$, ## $P < 0.01$, \$ $P > 0.05$. ($n = 3$ to 6)

we detected the expression of proliferation and migration related proteins in each group at the animal level. The results showed that Que had a certain inhibitory effect on the proliferation and migration related proteins PCNA and OPN in the pulmonary vessels of PAH rats. The corresponding protein changes were also detected in vitro, and the results were consistent with animal experiments. Que also had a significant inhibitory effect on the mRNA expression of proliferation and migration related proteins at the cell level. To sum up, Que can effectively inhibit the expression of proteins related to HPASMCs proliferation and migration, inhibit cell phenotypic transformation, and reverse pulmonary vascular remodeling, which is consistent with the results of HE in small and medium-sized pulmonary arteries and the EDU, scratch and Transwell™ experiments in cells in the above animal experiments.

TGF- β 1-Smad2/Smad3 signaling pathway, as a member of TGF- β superfamily, plays different roles in cell proliferation, migration, differentiation, adhesion, death and other processes, as well as in embryonic development, formation of extracellular matrix, bone formation and reconstruction and other physiological processes [39, 47, 48]. Some studies have shown that in the classic TGF- β 1 pathway, TGF- β 1 can combine with T β R1 and T β R2 receptors on the cell surface to form trimer complexes, which can phosphorylate Smad2/3 itself in the cell and form complexes with Smad4 to promote nuclear translocation, and enter the nucleus to start the synthesis and secretion of factors related to proliferation and migration. Therefore, TGF- β 1-Smad2/Smad3 signaling pathway plays an indispensable role in the process of pulmonary artery remodeling [15, 38]. In the present study, Que inhibited the expression of TGF- β 1 and P-Smad2/Smad3 proteins in PAH model group, but had no significant effect on Smad2 and Smad3 mRNA levels, indicating that Que inhibited the phosphorylation of Smad2 and Smad3 by down-regulating the expression of TGF- β 1, thus playing a nuclear regulatory role. Previous studies of our research group have found that TGF- β 1 inhibitor SB431542 can inhibit the expression levels of TGF- β 1, P-Smad2 and P-Smad3 after the intervention of HPASMCs, exert an inhibitory effect on the expression of proteins related to proliferation, migration and phenotypic transformation in HPASMCs, and affect PAH pulmonary vascular remodeling [15]. Combined with our experimental results, it can be concluded that quercetin may affect the proliferation, migration and phenotypic transformation of HPASMCs by regulating the TGF- β 1-Smad2/Smad3 signaling pathway. To sum up, through the establishment of the SD rat PAH model in vitro and the cultivation of HPASMCs model in vitro, this topic proved that Que can inhibit the

proliferation and migration of HPASMCs by regulating TGF- β 1-Smad2/Smad3 pathway, thereby inhibiting pulmonary vascular remodeling, and playing a protective role on PAH. However, as a new drug for the treatment of PAH, the specific pathway through which it affects the TGF signaling pathway has not been represented in this study and needs to be investigated in our next step.

Conclusion

Que may inhibit HPASMCs proliferation, migration and phenotypic transformation through TGF- β 1-Smad2/3 signaling pathway, thus playing a protective role in pulmonary vascular remodeling in PAH.

Abbreviations

DMEM	Dulbecco's modified Eagle's medium
FBS	Fetal Bovine Serum
FITC	Fluorescein isothiocyanate
HE	Hematoxylin and eosin
HPASMC	Human Pulmonary Artery Smooth Muscle cells
IF	Immunofluorescence
LV	Left Ventricular
MCT	Monocrotaline
mPAP	Mean Pulmonary Artery Pressure
mRNA	Messenger Ribonucleic Acid
OPN	Osteopontin
PAAT	Pulmonary Artery Acceleration Time
PASMCs	Pulmonary Artery Smooth Muscle cells
PCNA	Proliferating Cell Nuclear Antigen
PDGF-BB	Platelet derived growth factor-BB
PAH	Pulmonary Arterial Hypertension
α -SMA	Alpha- Smooth Muscle Actin
PVDF	Polyvinylidene fluoride
qRT-PCR	Quantitative Reverse Transcription PCR
Que	Quercetin
RV	Right Ventricular
RVH	Right Ventricular Hypertropahy
RVHI	Right Ventricular Hypertropahy Index
TGF- β 1	Transforming Growth Factor beta one
WA	Vessel Wall Area / Total Vascular Area
WT	Vessel Wall Thickness/Total Vascular Diameter

Supplementary Information

The online version contains supplementary material available at <https://doi.org/10.1186/s12872-024-04192-4>.

Additional file 1: Supplementary Fig. 1. Effects of different concentrations of PDGF-BB on OD value and proliferation rate of HPASMCs at 450 nm. Statistics of OD values of different concentrations of PDGF-BB at 450nm; Effect of different concentrations of PDGF-BB on proliferation rate of HPASMCs. 5 vs 0, * $P < 0.05$, 10 vs 0, ** $P < 0.01$, 20 vs 0, *** $P < 0.001$; 5 vs 2.5, # $P < 0.05$, 10 vs 2.5, 80 vs 2.5, ## $P < 0.01$, ### $P < 0.001$; 20 vs 2.5, 40 vs 2.5; $^{55}P < 0.01$.

Additional file 2: Supplementary Fig. 2. Effects of different concentrations of Que on the OD value and inhibition ratio of HPASMCs at 450 nm. Statistics of OD values of different concentrations of Que at 450nm; Effect of different concentrations of Que on inhibition rate of HPASMCs. 15 vs 0, * $P < 0.05$, 30 vs 0, 120 vs 0, ** $P < 0.01$, 60 vs 0, 90 vs 0, *** $P < 0.001$; 30 vs 15, # $P < 0.05$, 60 vs 15, 90 vs 15, 120 vs 15, ### $P < 0.001$, 90 vs 60; $^{5}P < 0.05$.

Acknowledgements

Permission has been secured from the person mentioned in the acknowledgements section.

Authors' contributions

Rui-Juan Gao: Study Design, Data Collection, Manuscript Preparation. Nigala Aikeremu: Data Collection, Data Interpretation. Nan Cao: Study Design, Data Collection. Chong Chen: Statistical Analysis, Literature Search. Ke-Tao Ma: Literature Search, Funds Collection. Li Li: Data Interpretation, Manuscript Preparation. Ai-Mei Zhang: Manuscript Preparation, Literature Search. Jun-Qiang Si: Study Design, Funds Collection.

Funding

The present study was supported by grants from the National Natural Science Foundation of China (grant nos.81560081), Guiding science and technology project of Xinjiang Production and Construction Corps, Xinjiang, China (No. 2022ZD004) and Project of Shihezi University First Affiliated Hospital (No. QN202208). The authors would like to thank Professor Ai-Mei Zhang and Professor Jun-Qiang Si from the Shihezi University for support in experiments.

Availability of data and materials

The datasets used and analysed during the current study are available from the corresponding author upon reasonable request.

Data availability

No datasets were generated or analysed during the current study.

Declarations

Ethics approval and consent to participate

This study was approved by the First Affiliated Hospital of Shihezi University. All methods were conducted in accordance with pertinent guidelines and regulations. All primary investigations included in this study obtained ethical approval from the relevant review board.

The study protocol was approved by the Ethics Committee of First Affiliated Hospital of Shihezi University. All animal experiments complied with the ARRIVE guidelines and were carried out in accordance with the Guidelines for Laboratory Animal Care and Use of the National Institutes of Health (NIH Publication No. 85–23).

Consent for publication

All the authors in this article agree to publish this article.

Competing interests

The authors declare no competing interests.

Author details

¹Department of Medical Imaging Center, First Affiliated Hospital of Shihezi University, Shihezi, Xinjiang 832002, China. ²Department of Physiology, Shihezi University School of Medicine, Xinjiang, North Second Road, Shihezi, Xinjiang 832000, China. ³Department of Physiology, Kangda College of Nanjing Medical University, Lianyungang, Jiangsu 222061, China. ⁴Department of Intensive Care Medicine, the Third People's Hospital of Xinjiang Autonomous Region, Urumqi, Xinjiang 830000, China. ⁵Key Laboratory of Xinjiang Endemic and Ethnic Diseases, Ministry of Education, Shihezi University School of Medicine, Shihezi, Xinjiang 832002, China. ⁶NHC Key Laboratory of Prevention, and Treatment of Central Asia High Incidence Diseases, First Affiliated Hospital, Shihezi University School of Medicine, Shihezi, Xinjiang 832002, China. ⁷Department of Physiology, Medical College of Jiaxing University, Jiaxing 314001, China. ⁸The 3rd Department of Cardiology, First Affiliated Hospital of Shihezi University, Xinjiang 832002, China. ⁹Department of Physiology, Huazhong University of Science and Technology of Basic Medical Sciences, Wuhan 430070, China.

Received: 18 February 2024 Accepted: 12 September 2024

Published online: 04 October 2024

References

1. Jose A, Eckman MH, Elwing JM. Anticoagulation in pulmonary arterial hypertension: a decision analysis. *Pulm Circ*. 2019;9:2045894019895451.
2. Lei S, Peng F, Li ML, et al. LncRNA-SMILR modulates RhoA/ROCK signaling by targeting miR-141 to regulate vascular remodeling in pulmonary arterial hypertension. *Am J Physiol Heart Circ Physiol*. 2020;319:H377–91.
3. Bissierier M, Mathiyalagan P, Zhang S, et al. Regulation of the methylation and expression levels of the BMPR2 Gene by SIN3a as a Novel Therapeutic Mechanism in Pulmonary Arterial Hypertension. *Circulation*. 2021;144:52–73.
4. Courboulin A, Barrier M, Perreault T, et al. Plumbagin reverses proliferation and resistance to apoptosis in experimental PAH. *Eur Respir J*. 2012;40:618–29.
5. Wang SC. PCNA: a silent housekeeper or a potential therapeutic target. *Trends Pharmacol Sci*. 2014;35:178–86.
6. Kapur R, Kasetty G, Rebetz J, et al. Osteopontin mediates murine trans-fusion-related acute lung injury via stimulation of pulmonary neutrophil accumulation. *Blood*. 2019;134:74–84.
7. Scott T, Qin C, Drummond G, et al. Innovative anti-inflammatory and pro-resolving strategies for pulmonary hypertension: high blood pressure research council of australia award 2019. *Hypertension (Dallas, Tex : 1979)*. 2021;78(5):1168–84.
8. Zhu A, Wang S, Wang Y, et al. Role of P38-MAPK signal transduction pathway and effect of panax notoginsin in rats with hypoxic hypercapnia pulmonary hypertension. *Zhongguo Ying Yong Sheng Li Xue Za Zhi*. 2012;28(1):79–83.
9. Yi H, Peng H, Wu X, et al. The therapeutic effects and mechanisms of quercetin on metabolic diseases: pharmacological data and clinical evidence. *Oxid Med Cell Longev*. 2021;2021:6678662.
10. Yang D, Wang T, Long M, et al. Quercetin: its main pharmacological activity and potential application in clinical medicine. *Oxid Med Cell Longev*. 2020;2020:8825387.
11. Papakyriakopoulou P, Velidakis N, Khattab E, et al. Potential pharmaceutical applications of quercetin in cardiovascular diseases. *Pharmaceuticals (Basel)*. 2022;15: undefined.
12. Nwaeburu CC, Abukiwan A, Zhao Z, et al. Quercetin-induced miR-200b-3p regulates the mode of self-renewing divisions in pancreatic cancer. *Mol Cancer*. 2017;16:23.
13. Rajabi S, Najafipour H, JafarnejadFarsangi S, et al. Perillyl alcohol and Quercetin ameliorate monocrotaline-induced pulmonary artery hypertension in rats through PARP1-mediated miR-204 down-regulation and its downstream pathway. *BMC Complement Med Ther*. 2020;20:218.
14. Yue Y, Li YQ, Fu S, et al. Osthole inhibits cell proliferation by regulating the TGF- β 1/Smad/p38 signaling pathways in pulmonary arterial smooth muscle cells. *Biomed Pharmacother*. 2020;121:109640.
15. Cao N, Tang X, Gao RJ, et al. Galectin-3 participates in PSMC migration and proliferation by interacting with TGF- β 1. *Life Sci*. 2021;274.
16. Gao H, Chen C, Huang S, et al. Quercetin attenuates the progression of monocrotaline-induced pulmonary hypertension in rats. *J Biomed Res*. 2012;26:98–102.
17. He Y, Cao X, Liu X, et al. Quercetin reverses experimental pulmonary arterial hypertension by modulating the TrkA pathway. *Exp Cell Res*. 2015;339:122–34.
18. Zhao X, Bai X, Li J-L, et al. Sevoflurane improves circulatory function and pulmonary fibrosis in rats with pulmonary arterial hypertension through inhibiting NF- κ B signaling pathway. *Eur Rev Med Pharmacol Sci*. 2019;23:10532–40.
19. Urboniene D, Haber I, Fang YH, et al. Validation of high-resolution echocardiography and magnetic resonance imaging vs. high-fidelity catheterization in experimental pulmonary hypertension. *Am J Physiol Lung Cell Mol Physiol*. 2010;299:L401-12.
20. Zaky A, Zafar I, Masjoan-Juncos JX, et al. Echocardiographic, biochemical, and electrocardiographic correlates associated with progressive pulmonary arterial hypertension. *Front Cardiovasc Med*. 2021;8:705666.
21. Luan Y, Chao S, Ju ZY, et al. Therapeutic effects of baicalin on monocrotaline-induced pulmonary arterial hypertension by inhibiting inflammatory response. *Int Immunopharmacol*. 2015;26:188–93.
22. Chen M, Ding Z, Zhang F, et al. A20 attenuates hypoxia-induced pulmonary arterial hypertension by inhibiting NF- κ B activation and pulmonary artery smooth muscle cell proliferation. *Exp Cell Res*. 2020;390.
23. Luo L, Wu J, Lin T, et al. Influence of atorvastatin on metabolic pattern of rats with pulmonary hypertension. *Aging (Albany NY)*. 2021;13:11954–68.
24. Sun Z, Nie X, Sun S, et al. Long non-coding rna meg3 downregulation triggers human pulmonary artery smooth muscle cell proliferation and migration via the p53 signaling pathway. *Cell Physiol Biochem*. 2017;42:2569–81.

25. Peng X, Li HX, Shao HJ, et al. Involvement of calcium-sensing receptors in hypoxia-induced vascular remodeling and pulmonary hypertension by promoting phenotypic modulation of small pulmonary arteries. *Mol Cell Biochem*. 2014;396:87–98.
26. Zhao H, Wang Y, Zhang X, et al. miR-181b-5p inhibits endothelial-mesenchymal transition in monocrotaline-induced pulmonary arterial hypertension by targeting endocan and TGFBR1. *Toxicol Appl Pharmacol*. 2020;386:114827.
27. Huang H, Zhang P, Wang Z, et al. Activation of endothelin-1 receptor signaling pathways is associated with neointima formation, neoangiogenesis and irreversible pulmonary artery hypertension in patients with congenital heart disease. *Circ J*. 2011;75:1463–71.
28. Wang YY, Luan Y, Zhang X, et al. Proteasome inhibitor PS-341 attenuates flow-induced pulmonary arterial hypertension. *Clin Exp Med*. 2014;14:321–9.
29. Thomas M, Docx C, Holmes AM, et al. Activin-like kinase 5 (ALK5) mediates abnormal proliferation of vascular smooth muscle cells from patients with familial pulmonary arterial hypertension and is involved in the progression of experimental pulmonary arterial hypertension induced by monocrotaline. *Am J Pathol*. 2009;174:380–9.
30. He Y, Cao X, Guo P, et al. Quercetin induces autophagy via FOXO1-dependent pathways and autophagy suppression enhances quercetin-induced apoptosis in PASMCs in hypoxia. *Free Radic Biol Med*. 2017;103:165–76.
31. Zhao Y, Lv W, Piao H, et al. Role of platelet-derived growth factor-BB (PDGF-BB) in human pulmonary artery smooth muscle cell proliferation. *J Recept Signal Transduct Res*. 2014;34:254–60.
32. Li Y, Shao J, Song J, et al. MiR-34a-3p suppresses pulmonary vascular proliferation in acute pulmonary embolism rat by targeting DUSP1. *Biosci Rep*. 2022;42: undefined.
33. Shao Z, Wang B, Shi Y, et al. Senolytic agent Quercetin ameliorates intervertebral disc degeneration via the Nrf2/NF- κ B axis. *Osteoarthritis Cartilage*. 2021;29:413–22.
34. Chen F, Wang H, Lai J, et al. 3-Bromopyruvate reverses hypoxia-induced pulmonary arterial hypertension through inhibiting glycolysis: In vitro and in vivo studies. *Int J Cardiol*. 2018;266:236–41.
35. Zhao FY, Xu SL, Zhang CF, et al. PDGF mediates pulmonary arterial smooth muscle cell proliferation and migration by regulating NFATc2. *Mol Med Rep*. 2021;23: undefined.
36. Yu L, Tu Y, Jia X, et al. Resveratrol protects against pulmonary arterial hypertension in rats via activation of silent information regulator 1. *Cell Physiol Biochem*. 2017;42:55–67.
37. Nie X, Dai Y, Tan J, et al. α -Solanine reverses pulmonary vascular remodeling and vascular angiogenesis in experimental pulmonary artery hypertension. *J Hypertens*. 2017;35:2419–35.
38. Lambers C, Roth M, Zhong J, et al. The interaction of endothelin-1 and TGF- β 1 mediates vascular cell remodeling. *PLoS One*. 2013;8:e73399.
39. Li YX, Run L, Shi T, et al. CTRP9 regulates hypoxia-mediated human pulmonary artery smooth muscle cell proliferation, apoptosis and migration via TGF- β 1/ERK1/2 signaling pathway. *Biochem Biophys Res Commun*. 2017;490:1319–25.
40. He RL, Wu ZJ, Liu XR, et al. Calcineurin/NFAT signaling modulates pulmonary artery smooth muscle cell proliferation, migration and apoptosis in monocrotaline-induced pulmonary arterial hypertension rats. *Cell Physiol Biochem*. 2018;49:172–89.
41. Liu Y, Zhang J, Yi B, et al. Nur77 suppresses pulmonary artery smooth muscle cell proliferation through inhibition of the STAT3/Pim-1/NFAT pathway. *Am J Respir Cell Mol Biol*. 2014;50:379–88.
42. Cao H, Cheng C, Su T, et al. Quercetin inhibits HGF/c-Met signaling and HGF-stimulated melanoma cell migration and invasion. *Mol Cancer*. 2015;14:103.
43. Dhanaraj T, Mohan M, Arunakaran J. Quercetin attenuates metastatic ability of human metastatic ovarian cancer cells via modulating multiple signaling molecules involved in cell survival, proliferation, migration and adhesion. *Arch Biochem Biophys*. 2021;701:108795.
44. Liu Y, Tang Z, Lin Y, et al. Effects of quercetin on proliferation and migration of human glioblastoma U251 cells. *Biomed Pharmacother*. 2017;92:33–8.
45. Yamada N, Matsushima-Nishiwaki R, Kozawa O. Quercetin suppresses the migration of hepatocellular carcinoma cells stimulated by hepatocyte growth factor or transforming growth factor- α : Attenuation of AKT signaling pathway. *Arch Biochem Biophys*. 2020;682:108296.
46. Vivekanandhan S, Mukhopadhyay D. Genetic status of KRAS influences Transforming Growth Factor-beta (TGF- β) signaling: an insight into Neuropilin-1 (NRP1) mediated tumorigenesis. *Semin Cancer Biol*. 2019;54:72–9.
47. Yao L, Shao W, Chen Y, et al. Suppression of ADAM8 attenuates angiotensin II-induced cardiac fibrosis and endothelial-mesenchymal transition via inhibiting TGF- β 1/Smad2/Smad3 pathways. *Exp Anim*. 2022;71:90–9.
48. Dobaczewski M, Chen W, Frangogiannis NG. Transforming growth factor (TGF)- β signaling in cardiac remodeling. *J Mol Cell Cardiol*. 2011;51:600–6.

Publisher's Note

Springer Nature remains neutral with regard to jurisdictional claims in published maps and institutional affiliations.